

PRACTICAL DOA ESTIMATION VIA A NETWORK OF DOA-BLIND SENSORS

M. Guerriero, P. Willett

University of Connecticut
ECE Department
Storrs, CT 06269 USA

S. Marano, V. Matta

University of Salerno
DIIE Department
Fisciano (SA), 84084 Italy

ABSTRACT

We consider the problem of DOA (Direction Of Arrival) estimation of an acoustic wavefront by a Wireless Sensor Network (WSN) within the SENMA architecture (a Mobile Agent (MA) repeatedly polls the sensors lying inside its field of view). The sensors, which are random in number and location, are DOA-blind and simply emit a pulse train synchronized to the acoustic event's passage; taken in aggregate, however, the MA can exploit its non-isotropic field of view (FOV) to infer an accurate DOA. In this paper we (i) use a more realistic "soft" FOV; (ii) account for multiple sources; and (iii) suggest a strategy for the MA. We find that the presence of more than one source can *improve* DOA estimation, and also that an optimal strategy for the MA *squints* near the expected DOA, as opposed to directly at it.

Index Terms— Wireless Sensor Network (WSN); Sensor Networks with Mobile Agent (SENMA); Multiple DOA Estimation; Dumb Sensors.

I. INTRODUCTION

The problem of estimating the Direction Of Arrival (DOA) of an acoustic planar wavefront using a Wireless Sensor Network (WSN) within the SENMA architecture (Sensor Network with Mobile Agents, [1]) has been dealt in some recent papers [2], [3]. A distinct feature of the approach pursued in [2], [3] was that individual sensors (also referred to as *nodes*) of the network are completely blind to DOA: they have no possibility of recognizing the DOA of an impinging acoustic wave, but they are only capable of sensing the acoustic signal and of recording the impinging time instant.

The key point is that they do not transmit bits of data but simply emit an analog periodic signal made of short pulses. In aggregate, they form a train of delta-like pulses, and this is what the rover observes. After an appropriate number of network polls, the MA can estimate the desired DOA based upon the concentration of the pulses in time, as in Fig. 2. A key feature of the MA is its eccentric field of view: an ellipse was used in [2], [3]. Here we extend that to a more

THIS RESEARCH WAS PARTIALLY SUPPORTED BY THE OFFICE OF NAVAL RESEARCH.

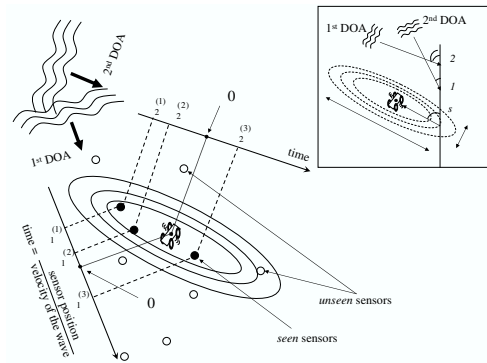


Fig. 1. The reference scenario.

realistic (*i.e.*, with smoother boundaries) the MA's field of view, and to multiple sources.

The reference scenario is depicted in Fig. 1. The DOAs are $\theta_i \in (0, \pi)$, $i = 1, 2$; later on, a MA polls the sensors within its field of view. At each snapshot the MA's field of view has a different and arbitrary orientation $\phi_s \in (0, 2\pi)$, with $s = 1, 2, \dots$, the snapshot index. It is convenient to model such a sequence $\{\phi_s\}$ as independent realizations of a random variable uniformly distributed in $[0, 2\pi)$. In any case we assume that successive dwells are *independent* of each other, in the sense that they always involve different sensors. Our paper is organized as follows. The probabilistic field of view and its impact on the single DOA estimation problem are discussed in section II. The multiple DOA estimation is presented in section III. The optimization of the MA orientation ϕ_s is discussed in Sect. IV. Suppressed mathematics are in [4].

II. SINGLE DOA ESTIMATION

II-A. Smooth field of view

In [2], [3] the rover's field of view has been considered *deterministic i.e.* in the sense that all the sensor lying inside were seen by the rover, while sensors lying outside were surely invisible. According with a more realistic scenario, the event that a sensor is visible or not is better modeled

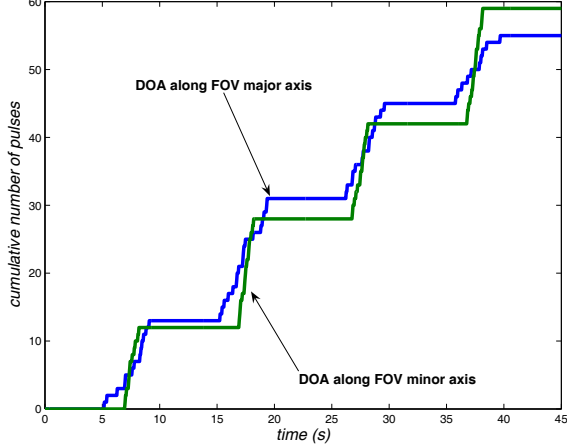


Fig. 2. The cumulative number of pulses versus time, for a DOA oriented to the FOV major and minor axes, reference figure 1. If the acoustic event travels along the *long/short* axis of the FOV the pulses are relatively diffused/concentrated in time.

as having a spatially-variant probability, rather than being on/off. Our choice for this probability is:

$$p(x, y) = \exp \left\{ -\frac{1}{2} \left[\frac{x^2}{\alpha^2} + \frac{y^2}{\beta^2} \right] \right\}, \quad (1)$$

where the positive constants α and β (we assume $\alpha \geq \beta$) determine the eccentricity of this *probabilistic* field of view and its rate of decaying to zero. The level curves of the above Gaussian-shaped probability are ellipses, see Fig. 1: this is a natural generalization of the model proposed in [2], [3], where a *deterministic* (i.e., on/off) ellipse was used.

II-B. Density of hitting times

Let us assume for the time being that a single acoustic wave impinges on the network, and let τ_i be the time instant that the i^{th} sensor is hit by the wavefront. Each MA's snapshot s corresponds to the vector of hitting times $\boldsymbol{\tau}_s = (\tau_1, \tau_2, \dots, \tau_{N_s})$. Depending on the chosen displacement and visibility of the sensors¹, it can be shown that the measured times τ_i s are independent samples from the following density

$$f_{\tau_i}(\tau) = \frac{1}{\sigma_s \sqrt{2\pi}} e^{-\frac{\tau^2}{2\sigma_s^2}}, \quad (2)$$

wherein

$$\sigma_s^2 = \frac{a_s^2 \alpha^2 + \beta^2}{(1 + a_s^2)v^2}, \quad (3)$$

with v being the velocity of sound, a_s being $\tan(\theta - \phi_s)$, and ϕ_s being the orientation of the MA at snapshot s .

¹It can be shown that the distribution of the sensors seen (i.e., polled and heard) by the rover forms an inhomogeneous spatial Poisson process.

II-C. ML Estimation and Fisher information

Recall that $\boldsymbol{\tau}_s$ is made of independent entries τ_i s: we have $\boldsymbol{\tau}_s \sim f_{\boldsymbol{\tau}_s}(\boldsymbol{\tau}_s) = \prod_{i=1}^{N_s} f_{\tau_i}(\tau_i)$, with $f_{\tau_i}(\tau_i)$ given by eq. (2). Times collected in successive snapshots are independent, but not identically distributed, as (2) depends on s through σ_s .

Since we cannot observe $\boldsymbol{\tau}_s$, but only t_s , we need the statistical characterization of the latter. Consider hence the N_s random variables $(\tau_1, t_2, t_3, \dots, t_{N_s}) = [\tau_1, \mathbf{t}_s]$. Their joint density is $F(\tau_1) = f_{[\tau_1, \mathbf{t}_s]}(\tau_1, t_2, t_3, \dots, t_{N_s}) = f_{\boldsymbol{\tau}_s}(\tau_1, t_2 + \tau_1, t_3 + \tau_1, \dots, t_{N_s} + \tau_1)$. We have

$$F(\tau_1) = \prod_{i=1}^{N_s} \frac{1}{\sigma_s \sqrt{2\pi}} \exp \left\{ -\frac{(t_i + \tau_1)^2}{2\sigma_s^2} \right\} \quad (4)$$

with $-\infty < \tau_1 < \infty$, and $f_{\mathbf{t}_s}(\mathbf{t}_s) = \int_{-\infty}^{+\infty} F(\tau_1) d\tau_1$.

Integrating eq. (4) with respect to τ_1 amounts to marginalizing an N_s -dimensional multivariate Gaussian density. The result is

$$f_{\mathbf{t}_s}(\mathbf{t}_s) = \frac{\exp \left(-\frac{1}{2} \mathbf{t}_s^T \mathbf{C}^{-1} \mathbf{t}_s \right)}{(2\pi)^{\frac{N_s-1}{2}} (\det \mathbf{C})^{1/2}}, \quad (5)$$

where $\mathbf{C} = \sigma_s^2 \mathbf{Z}$ and where we have defined the $(N_s - 1) \times (N_s - 1)$ covariance matrix

$$\mathbf{Z} = \begin{pmatrix} 2 & 1 & \dots & 1 \\ 1 & 2 & \dots & 1 \\ & & \ddots & \\ 1 & 1 & \dots & 2 \end{pmatrix}. \quad (6)$$

Clearly, \mathbf{C} depends upon the DOA θ only through σ_s^2 .

As M grows, $\hat{\theta}_{ML}$ attains its asymptotic properties of unbiasedness and efficiency [5]: $E[\hat{\theta}_{ML}] \rightarrow \theta$, and $\text{VAR}[\hat{\theta}_{ML}] \rightarrow I_M^{-1}(\theta)$. Here $I_M(\theta) = \sum_{s=1}^M J_s(\theta)$ is the M -snapshots Fisher information with respect to θ , which results in

$$I_M(\theta) = M(\bar{N} - 1 + e^{-\bar{N}}) \frac{(\sqrt{1 - \psi^2} - 1)^2}{\sqrt{1 - \psi^2}}. \quad (7)$$

Here M is the total number of snapshots, \bar{N} is the average number of sensors per single snapshot and $\psi = \sqrt{1 - (\beta/\alpha)^2}$ represents the eccentricity of the ellipses' family, namely the eccentricity of the MA's field of view.

From (7) we see that $I_M(\theta)$ is constant with respect to θ , grows linearly with M and approximately linearly with \bar{N} . It is also easy to show that $I_M(\theta)$ is an increasing function of the eccentricity parameter ψ . Monte Carlo results are shown in Fig. 3. We see that the ML estimator approaches the CRLB very quickly as the number of snapshots increases.

III. MULTIPLE-DOA ESTIMATION

In contrast with the previous setup [2], [3], we now assume that the communication protocol between sensors inside the field of view and MA enables this latter to recognize which signals come from which sensors: sensors

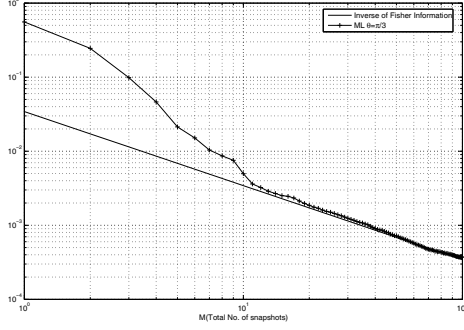


Fig. 3. Performance of the proposed estimator, in terms of the MSE $E[(\hat{\theta} - \theta)^2]$, compared to the Fisher proxy. In this example we have $v = 1$ m/s, $\alpha = 1$ m, $\beta = 0.3$ m, $\lambda = 10$ m $^{-2}$, resulting in $\bar{N} \approx 19$. Simulations are based on standard Monte Carlo counting process, involving 1000 runs for each point.

are identifiable. We now consider the joint estimation of multiple DOAs and, for simplicity, we only refer to the case of 2 DOAs.

Recall that τ_{ij} is the time instant when the i^{th} sensor is impinged upon by the plane wavefront of the j^{th} source. The joint pdf $f(\tau_{i1}, \tau_{i2})$ of the time instants τ_{i1} and τ_{i2} results in the following Gaussian density

$$f(\tau_{i1}, \tau_{i2}) = \frac{\exp\left\{-\frac{\frac{\tau_{i1}^2}{\sigma_{1s}^2} - 2\rho_s \frac{\tau_{i1}\tau_{i2}}{\sigma_{1s}\sigma_{2s}} + \frac{\tau_{i2}^2}{\sigma_{2s}^2}}{2(1-\rho_s^2)}\right\}}{2\pi\sigma_{1s}\sigma_{2s}(1-\rho_s^2)} \quad (8)$$

where

$$\begin{aligned} \sigma_{1s}^2 &= a^2\alpha^2 + b^2\beta^2, & \sigma_{2s}^2 &= c^2\alpha^2 + d^2\beta^2, \\ a &= \sin(\theta_1 - \phi_s)/v, & b &= \cos(\theta_1 - \phi_s)/v, \\ c &= \sin(\theta_2 - \phi_s)/v, & d &= \cos(\theta_2 - \phi_s)/v, \\ \rho_s &= \frac{aca^2 + bd\beta^2}{\sigma_{1s}\sigma_{2s}}. \end{aligned} \quad (9)$$

The key point is that the joint estimation of the two DOAs exploits the correlation between τ_{i1} and τ_{i2} (where the subscripts 1 and 2 denote θ_1 and θ_2 respectively) that we have deliberately ignored previously. Recall that (τ_{s1}, τ_{s2}) is made up of independent entries τ_{i1} and τ_{i2} , thus the complete statistical characterization of the joint vector (τ_{s1}, τ_{s2}) is $f(\tau_{s1}, \tau_{s2}) = \prod_{i=1}^{N_s} f(\tau_{i1}, \tau_{i2})$. At each snapshot the MA can only observe $2(N_s - 1)$ relative times. Taking for instance as reference τ_{11} and τ_{12} , the observables become $(\mathbf{t}_{s1}, \mathbf{t}_{s2}) = (t_{21}, t_{31}, \dots, t_{N_s-1}, t_{22}, t_{32}, \dots, t_{N_s-2})$. The distribution of the joint vector $\mathbf{t}_{s12} = (\mathbf{t}_{s1}, \mathbf{t}_{s2})$ results in a $2(N_s - 1)$ -dimensional multivariate Gaussian density

$$f_{\mathbf{t}_{s12}}(\mathbf{t}_{s12}) = \frac{\exp\left(-\frac{1}{2}\mathbf{t}_{s12}^T \Sigma^{-1} \mathbf{t}_{s12}\right)}{(2\pi)^{\frac{2(N_s-1)}{2}} (\det \Sigma)^{1/2}}, \quad (10)$$

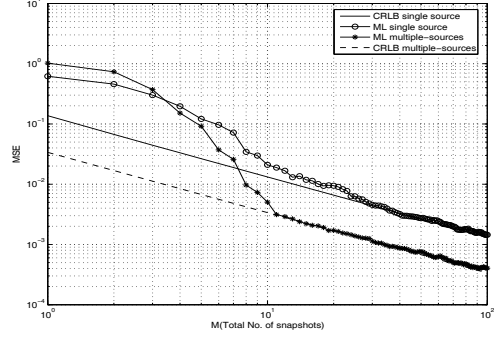


Fig. 4. Single DOA versus joint ML estimation procedures. In this example we have $v = 1$ m/s, $\alpha = 1$ m, $\beta = 0.3$ m, $\lambda = 3$ m $^{-2}$, $\bar{N} \approx 6$, $\theta = (\theta_1, \theta_2) = (\pi/3, \pi/6)$. The MSE of $\hat{\theta}_1$ is compared to its lower bound and to the performances of the single DOA approach. Simulations are based on standard Monte Carlo counting process, involving 1000 runs for each point.

having $2(N_s - 1) \times 2(N_s - 1)$ covariance matrix of the form

$$\Sigma = \begin{pmatrix} \mathbf{C}_1 & \vdots & \mathbf{C}_\rho \\ \dots & \dots & \dots \\ \mathbf{C}_\rho & \vdots & \mathbf{C}_2 \end{pmatrix}. \quad (11)$$

In the above we have introduced the $(N_s - 1) \times (N_s - 1)$ matrices $\mathbf{C}_1 = \sigma_{s1}^2 \mathbf{Z}$, $\mathbf{C}_2 = \sigma_{s2}^2 \mathbf{Z}$, $\mathbf{C}_\rho = \rho_s \sigma_{s1} \sigma_{s2} \mathbf{Z}$, and \mathbf{Z} is defined in eq. (6).

The matrix Σ depends upon the parameters θ_1 and θ_2 of the different DOAs through σ_{s1} , σ_{s2} and ρ_s , see eq. (9). The likelihood corresponding to M independent snapshots results in the product of the individual likelihoods, and the ML estimation $\hat{\theta}_{ML} = (\hat{\theta}_{1ML}, \hat{\theta}_{2ML})$ of the 2 DOAs is

$$\hat{\theta}_{ML} = \arg \max_{\theta} \prod_{s=1}^M f_{\mathbf{t}_{s12}}(\mathbf{t}_{s12}). \quad (12)$$

In the case of vector estimates, the concept of Fisher information generalizes to the Fisher Information Matrix (FIM) [5]. The FIM results in the symmetric form

$$I_M(\theta) = \frac{M}{4} (\bar{N} - 1 + e^{-\bar{N}}) \begin{pmatrix} \Lambda(\theta, \psi) & \Omega(\theta, \psi) \\ \Omega(\theta, \psi) & \Lambda(\theta, \psi) \end{pmatrix}, \quad (13)$$

where $\theta = (\theta_1, \theta_2)$, and the expressions of $\Lambda(\theta, \psi)$ and $\Omega(\theta, \psi)$ are not given for simplicity.

Due to the symmetric nature of the FIM in eq. (13), we note that, for a given θ , the MSE lower bounds of the two estimates $\hat{\theta}_1$ and $\hat{\theta}_2$ are the same. Thus, the performances of these two estimators approach the first diagonal entry of the inverse FIM which is given by

$$I_{M(1,1)}^{-1}(\theta) = \frac{1}{4M(\bar{N} - 1 + e^{-\bar{N}})} \left(-\frac{\alpha^4 - 6\alpha^2\beta^2 + \beta^4}{(\alpha^2 - \beta^2)^2} + \frac{\alpha^4 + 14\alpha^2\beta^2 + \beta^4}{\alpha^4 + 10\alpha^2\beta^2 + \beta^4 + 4\alpha^2\beta^2 \cos(2(\theta_1 - \theta_2))} \right).$$

When compared to the single DOA ML estimator, the performance improvements obtained by exploiting the data correlation are remarkable, as expected. An example of such comparison is offered in Fig. 4 where almost an order of magnitude is gained in terms of MSE. The reason for this improvement is that the *location* of each sensor within the FOV can be triangulated when there is more than one DOA: better inference becomes possible.

IV. OPTIMUM ROVER ORIENTATION

In [2] it was assumed that the rover travels across the network with iid uniform orientations $\{\phi_s\}_{s=1}^\infty$. We now investigate the performance improvement that can be achieved by optimizing the rover orientation ϕ_s at each snapshot s . The optimization criterion is based on maximizing the Fisher information $J_s(\theta, \phi_s)$ with respect to ϕ_s . It can be shown that ϕ_s^{opt} is given by

$$\phi_s^{opt} = \theta \pm \arctan\left(\frac{\beta}{\alpha}\right). \quad (14)$$

while $\phi_s = \theta$ (the rover always points towards the source) is the point of minimum of the Fisher information. Clearly, in order to select the optimal orientation ϕ_s one should know θ . In practice we can use its current estimate $\hat{\theta}_s$ instead. Thus, we can choose the following orientation strategy:

$$\begin{aligned} \phi_1^{opt} &= \pm \arctan\left(\frac{\beta}{\alpha}\right), \\ \phi_s^{opt} &= \hat{\theta}_{s-1} \pm \arctan\left(\frac{\beta}{\alpha}\right), \quad s > 1. \end{aligned}$$

As to the indeterminateness of the signs, for $s = 1$ the choice is arbitrary, and for $s > 1$ we alternatively switch between the two. Although one might at first blush believe that to point directly toward $\hat{\theta}_{s-1}$ it is apparently better to squint to the right or left: an intuitive explanation is that when the FOV is pointed directly *towards* the true DOA the derivative of both the spread and the concentration of “beeps” is zero. This derivative represents the sensitivity of the estimate to the measurement, and the nadir of each when either the major or minor axis is toward the true DOA.

Replacing ϕ_s with ϕ_s^{opt} , the Fisher information becomes

$$I_M^{opt}(\theta) = \frac{M}{2}(\bar{N} - 1 + e^{-\bar{N}}) \left(\frac{\psi^4}{1 - \psi^2} \right), \quad (15)$$

which verifies the fact that $I_M^{opt}(\theta) > I_M(\theta)$, $\forall \psi$.

Fig. 5 shows the MSE improvement with the optimized rover orientation, compared to uniformly chosen ϕ_s . Also shown is the MSE corresponding to a rover always pointed towards the source (*i.e.*, $\phi_s = \theta$); as expected the performance worsens.

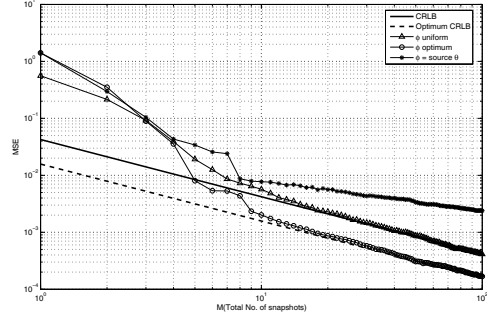


Fig. 5. Estimation MSE versus the number of snapshots. CRLB and optimum CRLB refer to the inverse of $I_M(\theta)$ and $I_M^{opt}(\theta)$, respectively (see eqs. (7) and (15)). We see that a uniform choice of ϕ_s asymptotically leads to $1/I_M(\theta)$, while the optimized strategy achieves $1/I_M^{opt}(\theta)$. For illustrative purposes, it is also shown that, as expected, choosing $\phi_s = \hat{\theta}$ leads to the worst performances. This example refers to $v = 1$ m/s, $\alpha = 1$ m, $\beta = 0.3$ m, $\lambda = 10$ m⁻², resulting in $\bar{N} \approx 19$. Simulations are based on standard Monte Carlo counting process, involving 1000 runs for each point.

V. CONCLUSIONS

Previously, we explained how a field of DOA-blind sensors might be made to estimate DOAs using the SENMA communication architecture. Here, we elaborate, in that

- we have shown that estimation is possible with the non-ideal FOV: in fact, the expressions are simpler;
- we have found that DOA estimation performance can be better for multiple than for single sources; and
- we have proposed a “sensor management” strategy for the MA to orient its FOV, with the discovery that the best orientation is neither directly toward the true DOA (or the current best estimate of it) nor away, but squinted at an oblique angle.

VI. REFERENCES

- [1] L. Tong, Q. Zhao, and S. Adireddy, “Sensor networks with mobile agents,” in *Proceedings of MILCOM 2003*, Boston MA, Oct. 2003.
- [2] S. Marano, V. Matta, P. Willett, and L. Tong, “Support-based and ML approaches to DOA estimation in a dumb sensor network,” *IEEE Trans. Signal Processing*, vol. 54, no. 4, pp. 1563–1567, Apr. 2006.
- [3] —, “Dumb isotropic sensors Can find DOAs,” in *Proc. IEEE International Conference on Acoustics, Speech, and Signal Processing (ICASSP 2005)*, Philadelphia, PA, USA, Mar. 2005.
- [4] M. Guerriero, S. Marano, V. Matta, and P. Willett, “Some aspects of DOA estimation using a network of blind sensors,” *IEEE Trans. Signal Processing*.
- [5] H. L. Van Trees, *Detection, Estimation, and Modulation Theory. Part I*. New York: John Wiley & Sons, Inc., 1968 (reprinted, 2001).